J Appl Electrochem (2008) 38:689–694
DOI 10.1007/s10800-008-9488-4

ORIGINAL PAPER

Effects of saccharin on the electrodeposition of Ni–Co nanocrystalline coatings

Sh. Hassani · K. Raeissi · M. A. Golozar

Received: 14 August 2007 / Revised: 25 December 2007 / Accepted: 18 January 2008 / Published online: 5 February 2008

Abstract Nickel–Co nanocrystalline coatings were electrodeposited onto a carbon steel substrate with and without saccharin addition. In the absence of saccharin, current density and adsorption of hydrogen complexes and/or intermediate components were distinguished as two effective parameters causing nanocrystalline electrodeposits. In the latter case, the growth active sites can be blocked easily at low current densities. By increasing the current density, a lower degree of adsorption was associated by a significant increase in surface diffusion of adions resulting in grain growth. Although, the nucleation rate is expected to increase with current density, it seems that the Ni–Co grain size is not reduced by the nucleation rate. Adsorption of saccharin molecules and/or decomposed sulfide species occurred in the saccharin contained bath, resulting in slow surface diffusion of adions. Therefore, finer grains were obtained which produced a smooth morphology instead of the pyramidal forms obtained in the absence of saccharin.

Keywords Ni–Co · Nanocrystalline coating · EIS · Electrodeposition · Adsorption

1 Introduction

Electrodeposited Ni–Co coatings are an important engineering material used widely in many fields. This is due to their unique properties, such as magnetic or magnetoresistive [1], heat conductive [2], good wear resistance and electrocatalytic activity [3]. Although Ni–Co coatings are mainly used in protective and plating applications, they are also used as permanent magnetic memories with a high commutation speed [4]. This alloy is used in various applications of magnetic devices, especially in microsystems technology to manufacture sensors, actucators, microrelays and inductors [5].

Nickel-Cobalt alloys form a complete solid solution over the whole composition range [6]. Investigations on electrodeposited Ni–Co alloys have shown that their microstructure and properties depend strongly on the Co content [3, 7]. Alloying the Ni with Co also improves its thermal stability [8]. Co content in electrodeposited Ni–Co coatings can be controlled by experimental parameters, such as bath composition, temperature, pH and current density [3, 7].

Saccharin, as an organic additive, has long been used in electroplating to reduce the internal stress of deposits and to refine the grain structure [9]. Saccharin molecules are adsorbed in a reversible way on active sites of the electrode surface, thereby blocking active sites and reducing crystal growth. Moreover, surface diffusion of the adatoms is impeded by adsorbed organic molecules [10]. Saccharin is especially effective in reducing residual stress and improving film quality [9].

Cziraki et al. [11] attributed the increasing grain size of nickel deposited from a nickel sulfate solution to a decrease in the concentration of Ni ions at the deposit-electrolyte interface. Ebrahimi et al. [12] showed that the efficiency of nickel deposition decreases with increasing current density, probably due to a relative decrease in the Ni ion concentration. Haug and Jenkins [13] have shown that hydrogen decreases the surface energy of {100} crystallographic planes preferentially and encourages planar growth in nickel. Therefore, it is plausible that the modification of the growth interface by hydrogen could facilitate the formation of larger grains.

Sh. Hassani · K. Raeissi (✉) · M. A. Golozar
Department of Materials Engineering, Isfahan University of Technology, Isfahan 84156-83111, Iran
e-mail: k_raeissi@cc.iut.ac.ir

Compared with conventional microcrystalline electrodeposited coatings, nanocrystalline electrodeposited coatings have a substantially higher strength, hardness and wear resistance. Normally, strengthening of polycrystalline materials by grain refinement is technologically attractive because it generally does not adversely affect ductility and toughness [14]. A recent investigation has shown that grain refining from microcrystalline to nanocrystalline Ni coatings in alkaline solution can improve corrosion resistance by increasing passive film resistance [15]. It has been shown that electrodeposition is a useful method for the preparation of novel nanocrystalline alloys or heterogeneous films of different metals and alloys for various applications [16]. The important role of grain size on the properties of Ni–Co nanocrystalline coatings led us to investigate the effect of various parameters such as applied current density and saccharin addition on nucleation and growth.

2 Experimental procedures

Carbon steel (AISI 1045) was used as substrate in a disk of 0.85 cm^2 surface area. The substrates were mechanically polished up to 600 grade abrasive paper and then electropolished in a solution containing 95% acetic acid and 5% perchloric acid solution for 2–3 min. Ni–Co alloy was electrodeposited from a typical Watts-type bath. The bath temperature was kept constant at 43 °C. The number of Coulombs passed was kept constant at 36 C. This led to a coating thickness of about 13 μm. The coating thickness was measured using cross-sections of coated specimens. The composition of the bath used is shown in Table 1.

The Ni–Co alloy was electrodeposited using graphite as an auxiliary anode with a saturated calomel reference electrode. Using dilute ammonia or dilute sulfuric acid, the pH of the bath was controlled and adjusted at 4.3. As an initial step, all polarization regions including: activation, activation-diffusion and diffusion zones were determined by direct cathodic sweeping of the potential. EIS measurements were carried out at five DC potentials selected based on the above mentioned polarization regions. These potentials were −850, −900, −1,080, −1,170 and −1,500 mV (Fig. 1). In order to measure the impedances, an EG&G AC responser

Table 1 Composition of the plating solution

Materials	Concentration/g l^{-1}
$NiSO_4 \cdot 6H_2O$	250
$CoSO_4 \cdot 7H_2O$	4
$NiCl_2 \cdot 6H_2O$	45
H_3BO_3	30
Saccharin	1

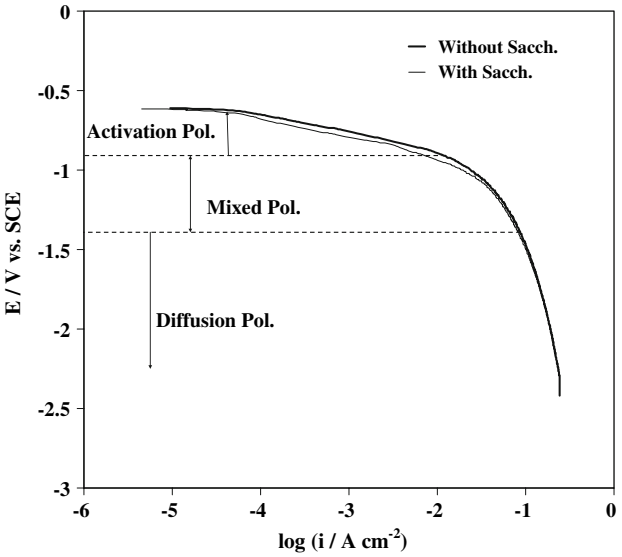

Fig. 1 Cathodic polarization plots obtained in baths with and without saccharin (scan rate = 40 mV s^{-1})

(model 1025) was coupled with an EG&G Potentiostat/Galvanostat (model 263A). The coatings were deposited in baths with and without saccharin addition at current densities corresponding to the above-mentioned potentials. A Philips XL30 Scanning Electron Microscope (SEM) was used to study the coating morphology. The presence of Co in the coatings was determined by EDS coupled with SEM. The grain size was determined using X-ray patterns obtained by X-ray diffraction (XRD, model X'pert Philips).

3 Results and discussion

3.1 Optimum current densities for coating deposition

Suitable current densities for electrodeposition were selected from cathodic polarization readings performed in baths with and without saccharin (Fig. 1). Three polarization regions including activation, mixed (activation + diffusion) and diffusion are seen. Current densities of 5 and 12 mA cm^{-2} from the activation polarization region, 39 and 55 mA cm^{-2} from the mixed polarization region and 104 mA cm^{-2} from the diffusion polarization region were selected for coating deposition. These current densities correspond to potentials of −850, −900, −1,080, −1,170 and −1,500 mV, respectively.

3.2 Grain size determination

X-ray diffraction patterns of the as-deposited and annealed Ni–Co alloy coatings are shown in Fig. 2. The annealing

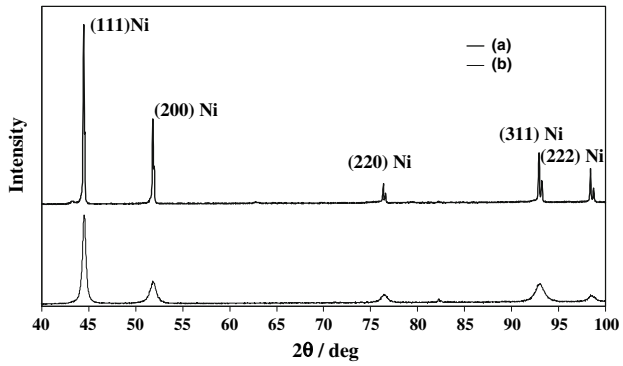

Fig. 2 XRD patterns corresponding to the (**a**) annealed and (**b**) as-deposited Ni–Co alloy

was performed for 15 min at 773 °C [17]. As seen in Fig. 2, in the case of annealing, the peaks are sharper indicating that grain growth has occurred. From the patterns obtained, a solid solution of face-centered cubic structure is deduced for Ni/Co coating.

Table 2 shows the grain size and cobalt content of coatings obtained at different current densities. The grain size was calculated using the angular width of the Nickel (111) peak at its Full-Width at Half Maximum (FWHM) in conjunction with the Scherrer equation [18]. The four-parameter Gaussian function was used for curve fitting analysis required for FWHM determination. Instrumental line broadening was also measured by a silicon standard specimen and corrected by the Gaussian–Cauchy equation. It has been shown that the grain size measured by the Gaussian–Cauchy equation is similar to what is obtained by TEM observations [15, 16].

Results indicate that the as-deposited coating from both baths (i.e., with and without saccharin) consisted of nanocrystalline grains (Table 2). It is also shown that in the solution with no saccharin, coarser grains are produced by increasing the current density. However, when saccharin is added to the bath, coating grain size is decreased (20 nm comparing to 36–56 nm), and remains almost constant at all current densities. In both cases, the cobalt content of the deposits decreases slightly with increasing current density. As seen from Table 2, the cobalt content of deposits obtained from bath without saccharin is more sensitive to current density variations.

3.3 EIS test results

In order to investigate the electrochemical reasons for nanocrystalline coating deposition, EIS tests were performed at −850, −900, −1,080, −1,170 and −1,500 mV (versus SCE) in baths with and without saccharin. These potentials correspond to current densities of 5, 12, 39, 55 and 104 mA cm^{-2}, respectively (Table 2). Nyquist plots obtained at the above potentials in baths with and without saccharin are shown in Figs. 3 and 4, respectively. In both baths, three time constants can be distinguished on the Nyquist plots at high cathodic potentials. The first time constant which appears as a capacitive loop at high frequencies belongs to double layer capacitance parallel to charge transfer resistance. The second and third time constants, which appear as inductive loops at lower frequencies, are most probably created due to the adsorption of hydrogen complexes and intermediate components, as also mentioned by other authors [4, 19].

Figure 5 shows the variation of charge transfer resistance with cathodic potential. The charge transfer resistances were extracted from the Nyquist plots in Figs. 3 and 4 by direct fitting a circle onto the high frequency capacitive loop. The diameter of this circle is considered as the charge transfer resistance. As seen from Fig. 5, the charge transfer resistance is reduced in both cases (i.e., with and without saccharin addition) with decrease in cathodic potential. The decrease in charge transfer resistance maybe related to the increase in surface diffusion of adions [14]. It has been proposed that a typical charge transfer takes place via three steps: ion transfer to terrace sites (step 1), surface diffusion of adions on terrace sites (step 2), and surface diffusion of adions on step-edge sites (step 3) [20]. It is well-known that increasing the surface diffusion of adions would facilitate its flux to the active growing sites (ex. kink sites) and thus accelerate

Table 2 Grain size and cobalt percentage of coatings obtained in baths with and without saccharin

Current density / mA cm^{-2}	Potential/ mV	Grain size/nm (bath with saccharin)	Cobalt percentage/ wt% (bath with saccharin)	Grain size/nm (bath without saccharin)	Cobalt percentage/wt% (bath without saccharin)
5	−850	21	8	35	6.8
12	−900	19	7.5	39	6.6
39	−1,080	20	5	43	5.5
55	−1,170	20	5	50	3.5
104	−1,500	19	5	56	3

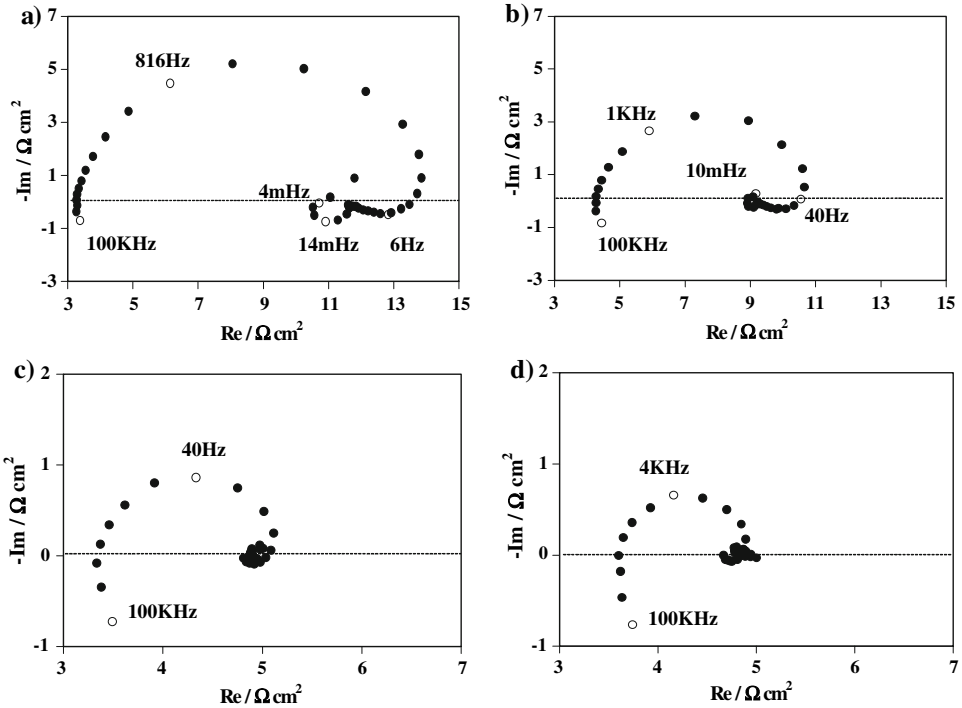

Fig. 3 Nyquist plots of Ni–Co alloy deposited from saccharin contained bath in (**a**) −850 mV, (**b**) −900 mV, (**c**) −1,080 mV and (**d**) −1,170 mV

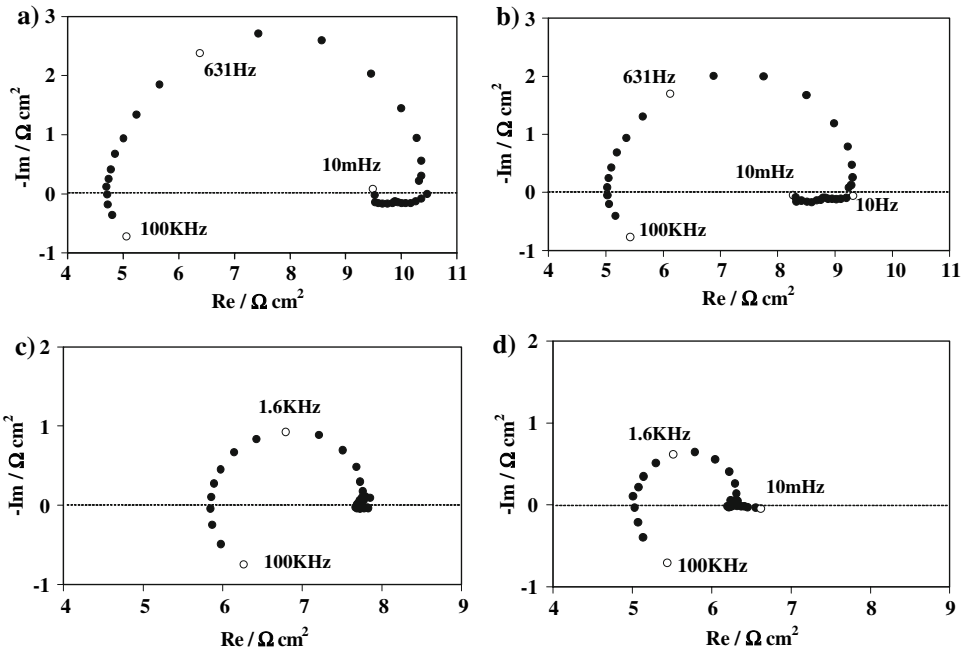

Fig. 4 Nyquist plots of Ni–Co alloy deposited from the bath without saccharin in (**a**) −850 mV, (**b**) −900 mV, (**c**) −1,080 mV and (**d**) −1,170 mV

the grain growth. Therefore, higher rates of grain growth, and thus larger grain size, are expected at lower cathodic potentials (i.e. higher current densities) [20, 21].

The second effect of decreasing the cathodic potential is the reduction of adsorption of electrochemical species. Referring to Figs. 3 and 4, two low frequency inductive loops are observed at high cathodic potentials in both baths. In the bath with no saccharin, these two inductive loops have been related to the adsorption of hydrogen complexes with metallic sources such as NiH^+, CoH^+ and intermediate components adsorption such as $NiOH^+$ and $CoOH^+$ [4], respectively in order of decrease in frequency. Adsorption of hydrogen complexes and intermediate components that are believed to occur onto the growing active sites can block them and thus stop grain growth [21]. By decreasing the cathodic potential in the bath with no saccharin, the diameter of the inductive loops is reduced and, finally, the loops disappear (Fig. 4). This means that

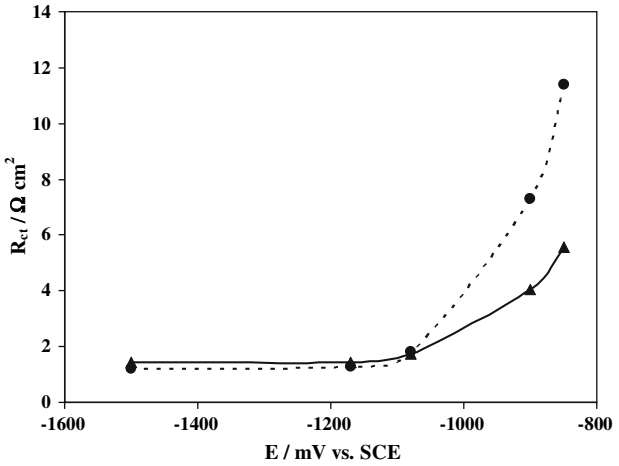

Fig. 5 Charge transfer resistance (Ω cm^2) versus cathodic potential in bath without (▲) and with saccharin (●)

the grain growth should be intensified by decreasing the cathodic potential, due to its influence in diminishing adsorption and therefore the blocking effect. This results in larger grain size. In the bath containing saccharin, it is observed that the inductive loop corresponding to hydrogen complex adsorption persists even at lower cathodic potentials (Fig. 3c, d). Therefore, decreasing the cathodic potential cannot have a significant effect on diminishing of the blocking effect occurring during electrodeposition. It seems that more stable adsorbed species formed in the presence of saccharin are responsible.

The third effective parameter influencing grain size is the nucleation barrier energy. This parameter is suggested by Volmer and Weber [22] and may also be affected by cathodic potential. The nucleation barrier energy is inversely proportional to the square of deposition overpotential, $(1/|\eta^2|)$, or inversely proportional to the deposition overpotential, $(1/|\eta|)$, for 3D and 2D nucleation, respectively [22]. Therefore, a higher rate of nucleation is expected with decreasing cathodic potential. It can thus be proposed that finer grains (produced through higher nucleation rate and lower rate of grain growth) are favored by increased charge transfer resistance, blocking the active growth sites and decreasing the activation energy for nucleation. Decreasing the cathodic potential (increasing the current density), decreases the activation energy for nucleation drastically and leads to a higher nucleation rate. This favors fine grain formation during deposition. However, at the same time, the charge transfer resistance and the adsorption tendency, which are responsible for preventing grain growth, are reduced by decreasing the cathodic potential and thus result in larger grains. It seems that competition between the two above mentioned effects, resulting from decreased cathodic potential (due to increasing the current density), leads to coarser grains at lower cathodic potentials in the bath with no saccharin, (see Table 2). In order to prevent grain growth satisfactorily, especially at higher current densities, saccharin can be used as an effective additive. The calculated grain size using XRD patterns and the Scherrer equation (Table 2), clearly confirms the effect of saccharin on grain size refining.

Saccharin can be adsorbed in both reversible and irreversible forms [16]. EIS shows that saccharin increases the charge transfer resistance, especially at high cathodic potentials (Fig. 5). This may be related to the reversible adsorption of saccharin molecules. Thus, saccharin can act as an obstacle to prevent surface diffusion of adions toward the active sites of growth (kink sites). Therefore, the growth rate is decreased and finer grains are obtained. Thus, saccharin molecules are adsorbed instead of water molecules attached to the cathode surface, probably because of their lower dipole torque than water molecules. This reduces the double layer capacitance value, as shown in Fig. 6. On the other hand, some saccharin molecules, which are adsorbed on the cathode surface, can be decomposed to other adsorbed sulfide-contained species [16]. This kind of adsorption is irreversible and shows inductive behavior in AC impedance readings. It is believed that at low cathodic potentials (i.e., in the diffusion polarization region), saccharin cannot be adsorbed in reversible form. For this reason, the Nyquist plots from both baths show the same charge transfer resistance at low cathodic potentials as seen in Fig. 5. It is believed that the sulfide-contained species adsorbed irreversibly at low cathodic potentials, can block active growth sites [16]. This has an additional inhibiting effect on grain growth, particularly at lower cathodic potentials (Fig. 3c, d). The significant effect of saccharin adsorption on increasing charge transfer resistance at higher cathodic potentials and its blocking effect at lower cathodic potentials are believed

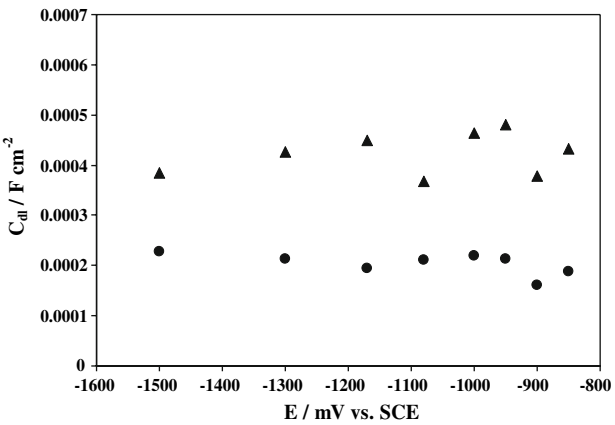

Fig. 6 Double layer capacitance (F cm^{-2}) versus cathodic potential in baths without (▲) and with saccharin (●)

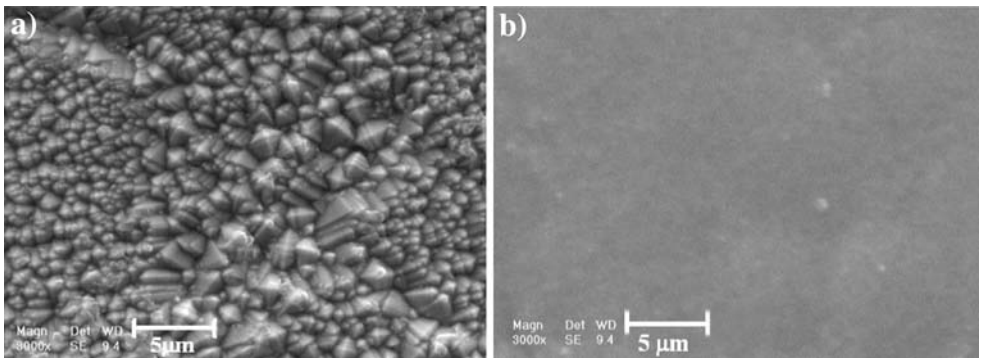

Fig. 7 Typical SEM micrographs of Ni–Co coatings produced in different baths at 12 mA cm^{-2}, (**a**) without saccharin, (**b**) with saccharin

to be the reasons for obtaining constant grain size, independent of current density (Table 2).

3.4 Morphological observations

Scanning electron microscope micrographs of the coatings produced in the bath with no saccharin addition show a pyramidal morphology (Fig. 7a). Addition of saccharin inhibits pyramidal growth and reduces roughness producing a bright surface (Fig. 7b).

4 Conclusion

1) In the absence of saccharin, increasing the current density encourages grain growth of Ni/Co electrodeposits, and thus coarser grains are observed. EIS results showed that the grain growth occurs by: (a) reducing the charge transfer resistance and thus increasing surface diffusion of adions and (b) preventing the adsorption of electrochemical species onto the active growth sites.
2) Addition of saccharin into the bath refines the grain size of Ni/Co electrodeposits. EIS shows that saccharin molecules can be adsorbed reversibly at high cathodic potential and cause an increase in the charge transfer resistance, which decreases the surface diffusion of adions toward the active growth sites and thus retards grain growth.
3) The presence of saccharin inhibits pyramidal growth and thus a very smooth, shiny surface is obtained.

References

1. Gomez E, Pane S, Valles E (2005) Electrochim Acta 51:146
2. Chi B, Li J, Yang X, Gong Y et al (2005) Int J Hydrogen Energy 30:29
3. Wang L, Gao Y, Xue Q, Liu H et al (2005) Appl Surf Sci 242:326
4. Orinakova R, Turonova A, Kladekova D et al (2006) J Appl Electrochem 36:957
5. Golodnitsky D, Rosenberg Yu, Ulus A (2002) Electrochim Acta 47:2707
6. Gomez E, Ramirez J, Valles E (1998) J Appl Electrochem 28:71
7. Correia AN, Machado SAS (2000) Electrochim Acta 45:1733
8. Hibbard GD, Aust KT, Erb U (2006) Mater Sci Eng A Struct Mater 433:195
9. Natter H, Hempelmann R (1996) J Phys Chem 100:19525
10. Natter H, Schmelzer M, Hempelmann R (1998) J Mater Res 13:1186
11. Cziraki A, Fogarassy B, Gerocs I et al (1994) J Mater Sci 29:4771
12. Ebrahimi F, Ahmed Z (2003) J Appl Electrochem 33:733
13. Haug K, Jenkins T (2000) J Phys Chem B 104:10017
14. Wang L, Gao Y, Xu T et al (2006) Mater Chem Phys 99:96
15. Wang L, Zhang J, Gao Y, Xue Q, Hu l, Xu T (2006) Scr Mater 55:657
16. Wu BYC (2002) Synthesis and characterization of nanocrystalline alloys in the binary Ni–Co system. B.Sc. thesis, University of Toronto
17. Wang GF, Chan KC, Zhang KF (2006) Scr Mater 54:765
18. Cullity BD, Stock SR, Stock S (2001) Elements of x-ray diffraction. Addision-Wesley, London
19. Gabrielli C (1998) Identification of electrochemical processes by frequency response analysis. Technical Report No. 004/83, University of Pierre et Marie Curie, Paris
20. Schlesinger M, Paunovic M (2000) Modern electroplating. John Wiley & Sons, London, p 46
21. El-Sherik AM (1995) J Mater Sci 30:5743
22. Budevski E, Staikov G, Lorenz WJ (2000) Electrochim Acta 45:2559